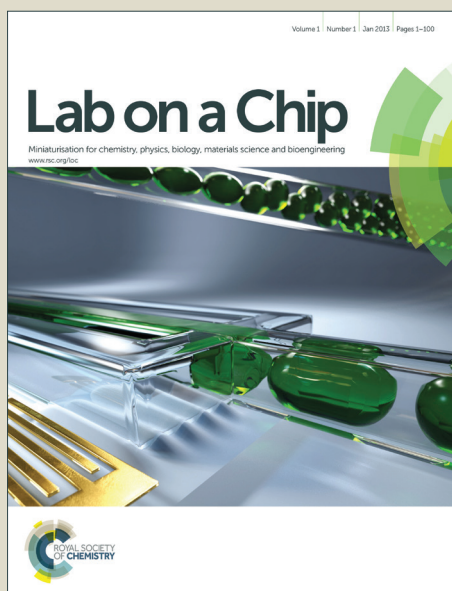


Lab on a Chip

Accepted Manuscript



This is an *Accepted Manuscript*, which has been through the Royal Society of Chemistry peer review process and has been accepted for publication.

Accepted Manuscripts are published online shortly after acceptance, before technical editing, formatting and proof reading. Using this free service, authors can make their results available to the community, in citable form, before we publish the edited article. We will replace this *Accepted Manuscript* with the edited and formatted *Advance Article* as soon as it is available.

You can find more information about *Accepted Manuscripts* in the [Information for Authors](#).

Please note that technical editing may introduce minor changes to the text and/or graphics, which may alter content. The journal's standard [Terms & Conditions](#) and the [Ethical guidelines](#) still apply. In no event shall the Royal Society of Chemistry be held responsible for any errors or omissions in this *Accepted Manuscript* or any consequences arising from the use of any information it contains.

1 Rapid and simple preparation of thiol- 2 ene emulsion-templated monoliths 3 and their application as enzymatic 4 microreactors

5 Josiane P. Lafleur,^{1*} Silja Senkbeil,¹ Jakub Novotny,^{2,3} Gwenaël Nys,⁴ Nanna
6 Bøgelund,¹ Kasper D. Rand,¹ Frantisek Foret,³ and Jörg P. Kutter¹

7
8 **Corresponding author: (+45) 3532 0398, Josiane.lafleur@sund.ku.dk*

9 *¹Department of Pharmacy, University of Copenhagen, Copenhagen, Denmark, ² Department
10 of Biological and Biochemical Sciences, University of Pardubice, Pardubice, Czech Republic,*

11 *³Institute of Analytical Chemistry of the ASCR, v.v.i., Brno, Czech Republic ⁴Pharmacy
12 Department, Université de Liège, Liège, Belgium*

13 Abstract

14 A novel, rapid and simple method for the preparation of emulsion-templated
15 monoliths in microfluidic channels based on thiol-ene chemistry is presented.
16 The method allows monolith synthesis and anchoring inside thiol-ene
17 microchannels in a single photoinitiated step. Characterization by scanning
18 electron microscopy showed that the methanol-based emulsion templating
19 process resulted in a network of highly interconnected and regular thiol-ene
20 beads anchored solidly inside thiol-ene microchannels. Surface area
21 measurements indicate that the monoliths are macroporous, with no or little
22 micro- or mesopores. As a demonstration, galactose oxidase and peptide-N-
23 glycosidase F (PNGase F) were immobilized at the surface of the synthesized
24 thiol-ene monoliths via two different mechanisms. First, cysteine groups on the
25 protein surface were used for reversible covalent linkage to free thiol functional
26 groups on the monoliths. Second, covalent linkage was achieved via free primary
27 amino groups on the protein surface by means of thiol-ene click chemistry and L-
28 ascorbic acid linkage. Thus prepared galactose oxidase and PNGase F
29 microreactors demonstrated good enzymatic activity in a galactose assay and the
30 deglycosylation of ribonuclease B, respectively.

31 Introduction

32 High surface area materials are essential in many chemical, biological and
33 analytical procedures. They can be used as solid supports for biomolecules in
34 enzymatic microreactors,¹⁻³ as stationary phases in chromatography^{4,5} and in
35 sample preparation steps such as extraction and pre-concentration.⁶
36 Commercially, sorbents are available as micrometer-sized beads made of
37 materials such as silica or agarose, which can either be bought pre-packed into

1 columns or packed manually. Optimal packing is not trivial to achieve and in
2 practice, even the best packed columns contain 30-40% void volume in addition
3 to the internal porosity of the beads.⁷ Packing columns in microfluidic chips is
4 even more challenging. Porous polymer monoliths offer an attractive alternative
5 to traditional packed beds. The processability of polymers can be used to easily
6 generate porous monoliths and beads from a mixture of monomers, free radical
7 initiators and porogenic solvents. Heterogeneous emulsions consisting of at least
8 one immiscible liquid dispersed in another in the form of droplets can be used as
9 templates for the production of porous materials, so-called emulsion-templated
10 monoliths, where either the dispersed or continuous phase is polymerized.⁸ In
11 the case of high internal phase emulsion templated monoliths (polyHIPEs), the
12 internal phase (usually forming more than 74% v/v of the emulsion), is dispersed
13 as discrete droplets within a continuous, less abundant external phase.⁹ These
14 monolithic materials can be prepared using a very simple process carried out
15 within the confines of a closed container, such as a microfluidic channel.
16 However, routine applications in microfluidic devices still face some challenges.
17 Poor adhesion of the monolith inside native unmodified polymeric
18 microchannels and monolith shrinkage are recurring problems. This can cause a
19 formed monolith to detach from the microchannel walls and create, for example,
20 large dead volumes. Therefore, the preparation of porous polymer monoliths and
21 their anchoring inside microfluidic channels is still an active area of research.

22 The attractive surface properties of thiol-ene (TE) polymers combined with
23 their ease of processing have made them an increasingly popular choice in the
24 fabrication of microfluidic devices for bioanalytical applications. Microfluidic
25 devices have been fabricated with commercially available TE-based photo-
26 curable adhesives (NOA, Norland Optical Adhesives, Norland Products Inc,
27 USA)¹⁰⁻¹⁶ as well as with custom formulations prepared in-house. Alterations in
28 the nature and/or stoichiometry of reactants in customized formulations
29 provide increased control over elastic modulus¹⁷ and surface chemistry.¹⁸
30 Carlborg *et al.*¹⁹ introduced a new class of TE materials, “off-stoichiometry” TE
31 (OSTE), achieved by altering extensively the stoichiometric ratios of the initial
32 reactant monomers. The result is a large excess of functional groups, either thiols
33 or enes, on the polymer surfaces and marked variations in material bulk
34 properties. The functional groups present at the surface of OSTE polymers have
35 been used as anchors for the covalent attachment of biomolecules^{20,21} and for
36 bonding.^{22,23}

37 Although TE-based microfluidic devices have received a high level of attention in
38 recent years, the ability of TE polymers to form in-chip porous monoliths
39 remains unexplored. The advantages of TE and OSTE in the preparation of
40 monoliths are numerous. The tunable OSTE surface chemistry can provide for a
41 simple means of covalently anchoring monoliths to microchannel walls without
42 any prior surface activation as well as for a wide variety of photoinitiated
43 functionalization reactions to occur at the surface of the monoliths. Moreover, the
44 TE click chemistry reaction²⁴⁻²⁶ offers high atom economy, a large
45 thermodynamic driving force and simple/mild reaction conditions²⁷ as well as
46 bio-orthogonality,²⁸ making it an ideal reaction scheme for the immobilization of
47 biomolecules on solid supports.^{20,21,29}

1 Immobilized enzyme microreactors are especially interesting since these tend to
2 exhibit much higher efficiency compared to the corresponding reactions in
3 solution.² A wide variety of chemical reactions are available for the
4 immobilization of biomolecules to TE solid supports. TE click chemistry allows
5 for simple and rapid photoinitiated modification of the solid support for the
6 covalent irreversible linkage of proteins through their amino groups.
7 Additionally, many enzymes and proteins possess free thiol groups at their
8 surface, which are available for interactions with the thiol groups present at the
9 surface of OSTE monoliths, allowing their straightforward and reversible
10 immobilization through direct disulfide linkage. Finally, in proteins where
11 cysteine residues form intramolecular disulfide bonds, immobilization can
12 proceed through thiol-disulfide exchange^{30,31} or photonic activation of disulfide
13 bridges.³² The thiol-disulfide exchange chemistry offers several advantages as
14 covalent disulfide bonds can form efficiently at neutral pH in aqueous solutions
15 and can be easily reversed with a reducing agent³³ for the regeneration of the
16 microreactor. TE and thiol-yne (TY) polyHIPEs have been prepared in bulk,³⁴⁻³⁸
17 with functional monomers added *in-situ*^{35,37} or in a post-functionalization step
18 performed on the ground monolith powder.³⁸ Droplet-based microfluidic devices
19 have been used to prepare NOA porous polymer microspheres³⁹ as well as
20 macroporous and non-porous TE/TY polymer beads.⁴⁰ In both cases, droplets
21 were cured individually and collected as beads from the microfluidic device.
22 Finally, Liu *et al.* used TE⁴¹ and TY⁴² photoinduced polymerization for the
23 preparation of macroporous monoliths in fused-silica capillaries for liquid
24 chromatography.

25 The method reported here allows monolith synthesis and anchoring inside TE
26 microchannels in a single and rapid photoinitiated step. We demonstrate that the
27 thus prepared monoliths can be post-functionalized reversibly through the
28 formation of disulfide bonds with enzymes or permanently using further
29 photoinitiated TE click chemistry to establish an irreversible covalent linkage to
30 enzymes via their free amino groups. As a demonstration, enzymatic
31 microreactors featuring immobilized galactose oxidase and PNGase F were
32 prepared and characterized by performing a galactose assay and the
33 deglycosylation of ribonuclease B, respectively.

34 **Experimental**

35 **Reagents**

36 Pentaerythritol-tetrakis(3-mercaptopropionate) (“tetrathiol”), Triallyl-1,3,5-
37 triazine-2,4,6(1H,3H,5H)-trione (“triallyl”), 2-(boc amino)ethanethiol, L-ascorbic
38 acid (ASA), galactose-oxidase from *Dactylium Dendroides* [50 U/ml], horseradish
39 peroxidase (HRP, lyophilized powder, 150 U/mg), PNGase F, ninhydrin, D-
40 galactose, D-(+)-glucose, , ribonuclease B (RNase B from bovine pancreas (50
41 Kunitz units/mg protein)), 10-acetyl-3,7-dihydroxyphenoxazine (ADHP), Tween
42 20 and 5,5'-dithiobis(2-nitrobenzoic acid) (DTNB) were obtained from Sigma
43 Aldrich (Brøndby, DK). Lucirin TPO-L (Ethyl-2, 4, 6-trimethylbenzoylphenyl
44 phosphinate) was obtained from BASF (Hardmatt, CH). Sylgard 184 –
45 poly(dimethylsiloxane) (PDMS) elastomer kit was obtained from Dow Corning

1 (Midland, MI, USA). Hypermer B246 and Span 80 surfactants were obtained from
2 Croda International Plc (Snaith, UK)

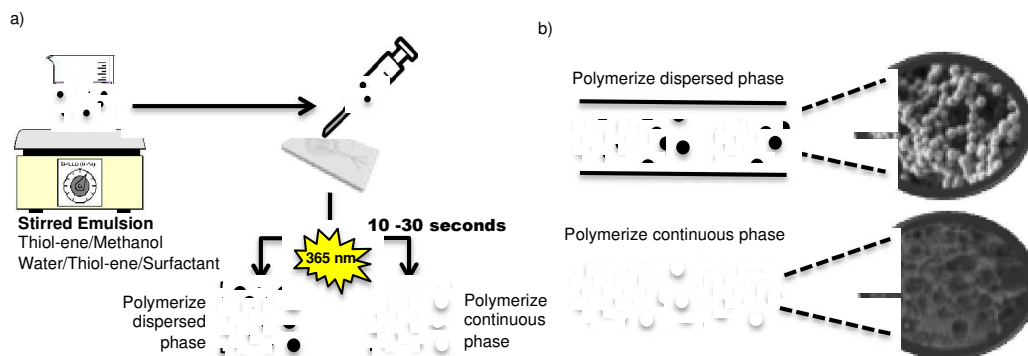
3 **Device fabrication**

4 A two-step replica molding process was used to fabricate the chips. Chip designs
5 were drawn with computer-aided-design software (Autodesk Inventor
6 Professional 2014, San Rafael, CA, USA). The devices featured channels 500 μm
7 wide by 200 μm deep. Chips used for fluorescence measurements featured an
8 800 μm deep detection chamber. The internal volume of the chips was 5 μl .
9 Micromilled poly(methylmethacrylate) (PMMA) masters as well as
10 poly(tetrafluoroethylene) chip holders featuring injection ports were
11 manufactured by high precision milling (Minitex 3, Minitex Machinery Corp.,
12 Norcross, GA, USA). PDMS molds for TE casting were prepared from the PMMA
13 masters and cured at 80°C for 2 hours.

14 The TE monomers (tetrathiol and triallyl) were mixed in various stoichiometric
15 ratios and poured into PDMS molds prior to exposure to UV light (25 s, 160
16 mW/cm^2 at 365 nm, Dymax EC 5000 Series UV curing flood lamp, Dymax Corp,
17 Torrington, CT). After curing, the TE parts were peeled off from the soft PDMS
18 molds. No photoinitiator was used to minimize chip auto-fluorescence. The
19 absence of photoinitiator was compensated for by the high output of the UV
20 flood lamp at wavelengths below 300 nm. Microfluidic chips were bonded
21 immediately after production, while a thin layer of uncured TE is still present at
22 the surface of the TE parts due to the short exposure time and slight oxygen
23 inhibition in the absence of photoinitiator. Prior to bonding, the TE parts were
24 warmed up for 10 minutes in an oven at 80°C and placed in conformal contact. A
25 slight pressure was applied on the assembly to ensure uniform sealing and it was
26 exposed to UV light (2 x 1 min, 160 mW/cm^2 at 365 nm) for bonding. The
27 bonded microfluidic chip was placed in an oven under a weight (80°C for 2
28 hours) and allowed to cool overnight before use. The final heating step helps
29 keep the parts soft and in contact with each other to further enhance the
30 bonding.

31 **Monoliths preparation**

32 Two different types of emulsions were prepared in order to form various in-chip
33 TE monoliths (Figure 1). The emulsions were prepared with either water or
34 methanol as the porogen, resulting in markedly different monolith morphologies.
35 The monomeric composition of the organic phase of the emulsions consisted of
36 stoichiometric TE (S-TE), off-stoichiometric TE featuring 40% excess thiol
37 groups (OSTE-thiol) or off-stoichiometric TE featuring 40% excess allyl groups
38 (OSTE-allyl). The monolith formation conditions are summarized in Table 1.



1
2 **Figure 1.** Monolith preparation procedure. a) The emulsions are stirred with a magnetic mixer or an
3 overhead mixer prior to injection in a TE microfluidic chip and exposure to UV light. b) Depending on the
4 surfactant and porogen present in the emulsion, the TE forms either the dispersed or the continuous phase.

5 **Table 1. Summary of the monolith formation conditions. All monolith emulsions contained 0.2% v/v**
6 **Lucirin TPO-L as a photoinitiator and were cured 7- 20 s (20.5 mW/cm² at 365 nm)**

Stirring conditions	Stirring time	Porogen	Surfactant	Polymer Phase	Experiments performed
Interconnected beads (polymerized dispersed phase)					
MS ¹ 40% of max. speed	1 min	60% w/w methanol	none	S-TE OSTE-Allyl OSTE-Thiol	Specific surface area
MS ¹ 40% of max. speed	1 min	80% w/w methanol	none	S-TE OSTE-Allyl OSTE-Thiol	Specific surface area, SEM, Enzyme immobilization, removal of enzymes bound through thiols with TCEP
MS ¹ 60% of max. speed	1 min	80% w/w methanol	none	S-TE OSTE-Allyl OSTE-Thiol	SEM
polyHIPE (polymerized continuous phase)					
MS ¹ 40% of max. speed		75% w/w Water	10% w/w Span 80	S-TE + 50% w/w CHCl ₃	(Unstable emulsions)
MS ¹ 40% of max. speed	Dropwise addition of water. Stirred	80% w/w Water	3% w/w Span 80	S-TE + 50% w/w CHCl ₃	(Unstable emulsions) SEM
MS ¹ 40% of max. speed	until the water was fully	80% w/w Water	20% w/w Span 80	S-TE + 50% w/w CHCl ₃	(Unstable emulsions)
OH ² 500 rpm	incorporated	80% w/w Water	10% w/w Span 80	S-TE + 50% w/w CHCl ₃	(Unstable emulsions)
OH ² 500 rpm	into the emulsion (3-	75% w/w Water	10% w/w Hypermer B246	S-TE + 50% w/w CHCl ₃	(Unstable emulsions)
OH ² 300 rpm	10 min).	80% w/w Water	3% w/w Hypermer B246	S-TE + 50% w/w CHCl ₃	(Unstable emulsions)

7 ¹Magnetic stirring, ²Overhead stirring

8 TE emulsions with water as the dispersed phase

9 Water (75-80% w/w) was added drop-wise to a TE mixture containing a
10 surfactant (Hypermer B246 or Span 80, 3-20% w/w of organic phase) and stirred
11 using an overhead stirrer (300-500 RPM, 3-10 minutes) in order to create an
12 emulsion with water as the dispersed phase. In some cases, chloroform was
13 added to the organic phase (50% w/w). Photoinitiator (0.2 % v/v Lucirin TPO-L)
14 was added to the mixture prior to injection in a TE microfluidic channel followed
15 by curing under UV collimated light (20 seconds, 20.5 mW/cm² at 365 nm, LS-
16 100-3C2 near UV light source, Bachur & Associates, Santa Clara, CA, USA).
17 Sections of the microfluidic chip where no monolith was desired were masked

1 prior to exposure. Unreacted monomers were removed by rinsing thoroughly
2 with distilled deionized water (DDW).

3 **Methanol emulsions with TE as the dispersed phase**

4 TE/methanol mixtures were magnetically stirred (60-80% w/w methanol, 1 min
5 magnetic stirring at constant speed) in order to create an emulsion with TE as
6 the dispersed phase. Photoinitiator (0.2% v/v Lucirin TPO-L) was added to the
7 mixture prior to injection in a TE microfluidic channel followed by curing under
8 UV collimated light (7-20 s, 20.5 mW/cm² at 365 nm). Sections of the
9 microfluidic channel where no monolith was desired were masked prior to
10 exposure. Unreacted monomers and methanol were removed by rinsing
11 thoroughly with DDW using a syringe pump (5 min at 10 µL/min). Microfluidic
12 channels were sealed prior to storage to avoid drying of the monolith.

13 **Monoliths characterization**

14 **Imaging and size distribution**

15 Microfluidic chips containing TE monoliths were pried opened and allowed to
16 dry thoroughly before Scanning Electron Microscope (SEM) imaging. The opened
17 microfluidic chips were taped to 12 mm studs with graphite tape for
18 conductivity. Samples were sputtered with gold (circa 4 nm) using a Cressington
19 Sputter Coater 108 (Cressington Scientific Instruments Ltd., Watford, UK) or a
20 Leica EM ACE 200 (Leica Microsystems GmbH, Wetzlar, Germany) and imaged
21 using a TM3030 benchtop SEM (Hitachi High-Technologies Europe GmbH,
22 Krefeld, Germany) or an XL 30 FEG-SEM (Philips FEI, Oregon, USA). Particle size
23 distribution was determined by measuring the diameter of the individual beads
24 with ImageJ (ImageJ, U. S. National Institutes of Health, Bethesda, MD, USA) with
25 N=119-241 measured beads per sample. The means of the distribution were
26 compared by performing a single factor ANOVA test (alpha = 0.05).

27 **Surface area analysis**

28 TE monoliths (S-TE as the dispersed phase, 60% and 80% methanol emulsions)
29 were prepared in bulk and cured as pellets in Eppendorf Tubes.[®] Gas (krypton)
30 adsorption measurements were performed at 77K using a Quantachrome
31 Autosorb-1 Sorption Analyzer (Quantachrome GmbH & Co, Odelzhausen,
32 Germany) and the specific surface area was determined by Brunauer-Emmett-
33 Teller (BET) analysis. Prior to the measurements, bulk monolith samples were
34 degassed under vacuum (40 °C, <10⁻³ torr) for 24 hours. For all samples, the BET
35 plots were linear (R² > 0.999) in the relative pressure range of 0.1 < P/P₀ < 0.3,
36 confirming the applicability of the BET equation. The specific surface area was
37 determined from the krypton adsorption isotherm using the BET equation.⁴³

38 **Thiol surface density**

39 The surface thiol density was quantitated using DTNB in a protocol adapted from
40 Ellman's procedure for quantifying free sulfhydryl group in solution⁴⁴ and
41 described elsewhere.²⁰ Briefly, thiol-ene slabs (20 mm × 20 mm × 0.5 mm, 60%
42 excess allyl - 60% excess thiols) were immersed in 5,5'-Dithiobis(2-nitrobenzoic
43 acid) (0.08 mg/mL in 0.1 M sodium phosphate buffer, pH 8.0). After 10 minutes,

1 the thiol-ene slab was removed and the absorbance of the solution was
 2 measured at 412 nm. The number of thiols on the surface of the thiol-ene slabs
 3 was evaluated from the molar extinction coefficient of TNB²⁻ ($14\,150\text{ M}^{-1}\text{cm}^{-1}$).⁴⁵

4 Enzyme immobilization

5 Two different immobilization schemes were used to link the enzymes to the
 6 monoliths. Table 2 summarizes the enzyme immobilization experiments
 7 performed.

8 **Table 2. Summary of the enzyme immobilization experiments. All monoliths were prepared from**
 9 **emulsions where TE forms the dispersed phase (interconnected beads) with 80% w/w methanol as**
 10 **the continuous phase, 0.2% v/v Lucirin TPO-L as the photoinitiator and magnetic stirring for 1 min**
 11 **(40% of max. stirring speed).**

Immobilized Enzyme	Monolith curing time ¹	Monolith Composition	Immobilization Scheme
Galactose oxidase	7s	OSTE-allyl (40% excess ene)	TE click chemistry ¹ and ASA linkage
Galactose oxidase	7s	OSTE-allyl (40% excess ene)	Unmodified TE, overnight incubation with enzyme
Galactose oxidase	20s	OSTE-thiol (40% excess thiol)	Unmodified TE, overnight incubation with enzyme
Galactose oxidase	20s	S-TE	Unmodified TE, overnight incubation with enzyme
PNGase F	7s	OSTE-allyl (40% excess ene)	TE click chemistry ¹ and ASA linkage

12 ¹20.5 mW/cm² at 365 nm

13 Immobilization on unmodified TE monoliths

14 Immobilization on unmodified TE monoliths was achieved by applying the
 15 enzyme solution (1 mg/ml PNGase F in 50 mM ammonium bicarbonate buffer at
 16 pH 8.0, 0,14 mg/ml, 50 U/mL for galactose oxidase in 50 mM Tris-HCl buffer at
 17 pH 8.0) to the monolith and incubating overnight at 4°C.

18 Immobilization on OSTE-allyl monoliths via TE click chemistry and ASA linkage

19 Immobilization on OSTE-allyl monoliths was achieved using a two-step reaction
 20 scheme. Free amine groups were introduced at the surface of the monolith using
 21 a TE click photochemical reaction between the thiol group of cystamine and the
 22 excess ene groups at the surface of the OSTE monolith in a procedure adapted
 23 from Magenau *et al.*⁴⁶ The amine group of the cysteamine was protected with a
 24 tert-butoxycarbonyl (t-Boc) group to reduce thiolate formation and favor the TE
 25 click reaction. 200 µL of 2-(boc amino)ethanethiol containing 0,5% v/v
 26 photoinitiator (Lucirin TPO-L) was injected on the monolith. Channel sections
 27 where no functionalization was desired were masked prior to exposure under
 28 collimated UV light (30 seconds exposure, 20.5 mW/cm² at 365 nm). After
 29 exposure, unreacted products were removed by flushing with 0,05 % Tween 20
 30 in DDW (5 min, 50 µl/min).

31 Following the photografting step, deprotection of the amine groups to reveal an
 32 NH₂-functionalized monolith was achieved by flushing the monolith with dilute
 33 hydrochloric acid overnight (4M, 12 hours at 4 µl/min) using NeMESYS high
 34 precision syringe pumps (Cetoni GmbH, Korbußen, Germany). Deprotection
 35 conditions were optimized on TE slabs using a procedure adapted from Patton *et*
 36 *al.*⁴⁷ A 0.2% ethanolic ninhydrin solution was deposited on the deprotected TE

1 polymer and heated at 110°C for 7 minutes revealing a blue color in the presence
2 of free amine groups, indicating successful deprotection.

3 Galactose oxidase and PNGase F were subsequently covalently immobilized on
4 the NH₂-monoliths by means of an L-ascorbic acid (ASA) linkage in a procedure
5 adapted from Tiller *et al.*⁴⁸ The ASA can work as a di-keto coupling agent
6 between the free amine groups on the surface of the monolith and the free
7 primary amino groups of the enzymes to be immobilized. A solution of ASA (1%
8 w/v in methanol) was applied on the NH₂-monolith and the channel was sealed
9 and left to incubate for 30 minutes. Unreacted products were flushed with DDW
10 (5 min, 30 μL/min). The channels were then filled with enzyme solution
11 (galactose oxidase, 50 U/mL in DDW or PNGase F, 50 U/mL in DDW), sealed and
12 left to incubate (24 hours at 4°C). Unreacted enzymes were removed by rinsing
13 thoroughly with DDW using a syringe pump (5 min, 30 μL/min).

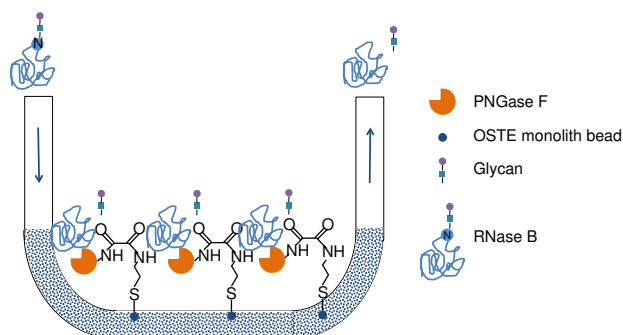
14 Reduction of disulfide bonds for enzyme removal

15 The monoliths featuring galactose oxidase were flushed for one hour at 50
16 μl/min with the reducing agent 2mM tris(2-carboxyethyl)phosphine (TCEP) to
17 remove enzymes immobilized via the formation of disulfide bonds.

18 Enzymatic reactions

19 Deglycosylation of ribonuclease B using the PNGase F microreactor

20 The PNGase F enzymatic microreactor was conditioned with ammonium
21 bicarbonate buffer (5 min at 30 μL/min). The denatured and reduced
22 glycoprotein solution (1 mg/ml ribonuclease B in 50 mM ammonium
23 bicarbonate buffer with 5 mM TCEP-HCl, heated to 100°C for 10 min) was
24 applied to the enzymatic microreactor and collected at the outlet using a vacuum
25 pick-up tool connected in series with a custom-made collection trap and a
26 vacuum pump. Similarly, batch mode samples were processed by mixing the
27 denatured and reduced ribonuclease B (20 μl, 1 mg/ml) with PNGase F (2 μl, 500
28 U/ml) for 2 hours at 37°C. The reaction was stopped by immersion in a hot water
29 bath (100°C, 5 min). The reaction scheme is illustrated schematically in Figure 2.



30
31 **Figure 2. Deglycosylation of RNase B on the enzymatic microreactor featuring PNGase F immobilized**
32 **via thiol-ene click chemistry and ASA linkage**

33 HPLC and mass spectrometry

34 The microreactor-deglycosylated ribonuclease B samples (50 pmol) were
35 injected manually onto a Waters Acquity HPLC system (Waters Corporation,

1 Milford, MA, USA) equipped with a 6-port switching valve (Rheodyne Model
2 7125) featuring an in-house packed microbore reversed-phase trap column (0.5
3 mm ID 2 mm, Poros 10 R1) in the sample loop. The trap column was pre-flushed
4 in load position by manual injection of formic acid (600 μ l, 0.23%), followed by
5 injection of the protein sample and finally washing of the trap column with
6 formic acid (800 μ l, 0.23%). Upon switching to the elute position, the protein
7 retained on the trap was eluted isocratically to the mass spectrometer (0.23%
8 formic acid in 90% acetonitrile, 0.040 ml/min).

9 Positive ion-electrospray ionization mass spectra were acquired on a Waters
10 SynaptG2 mass spectrometer (Waters Corporation, Milford, MA, USA) coupled to
11 the HPLC system. Mass spectra were processed using the MassLynx software
12 (Waters Corp, Milford, MA). The activity of PNGase F was assessed by comparing
13 the intensity of RNase peaks ($[M+15H]^{15+}$ for glycosylated and deglycosylated
14 species) from a non-deglycosylated sample as well as for samples subjected to
15 off-line and on-chip deglycosylation with PNGase F.

16 **D-galactose assay using the galactose oxidase enzymatic microreactor**

17 The galactose detection protocol was adapted from Sigma-Aldrich's galactose
18 assay (Galactose Assay Kit MAK012) and optimized for microfluidic application.
19 The microreactors were filled with the working solution (50 μ M D-galactose, 25
20 μ M 10-acetyl-3,7-dihydroxyphenoxazine (ADHP) and 0,01 U/ml HRP in tris/HCl
21 buffer, pH 8,0), and incubated (30 min at 37°C). D-galactose is oxidized into D-
22 galacto-hexodialdose by the monolith-immobilized enzyme producing hydrogen
23 peroxide. In the presence of hydrogen peroxide, HRP catalyses the oxidation of
24 non-fluorescent ADHP into the fluorescent product resorufin. The fluorescence
25 of resorufin (λ_{ex} 530-560 nm, λ_{em} 590 nm) was recorded with an inverted microscope
26 (IX71, Olympus Corporation, Tokyo, Japan) equipped with a Canon 550D (Tokyo,
27 Japan) digital camera. Images were acquired in 14 bit RAW format and image
28 analysis was performed with Matlab (MathWorks, Natick, MA, USA). All results
29 were blank corrected and normalized to a control (working solution and 50
30 U/ml galactose-oxidase).

31 Microreactors were stored 3-13 days in DDW (4°C) to assess the impact of
32 storage time on performance. The fluorescence intensity of resorufin obtained
33 before and after storage was compared. The ability of the microreactors to be re-
34 used was also evaluated. Microreactors were thoroughly washed (0,05% Tween
35 20 in DDW) to remove all the fluorescence products between each successive use
36 and re-used up to 5 times at 3-day intervals.

37 The immobilization and enzymatic reaction schemes performed on the
38 monoliths are summarized in Table 3.

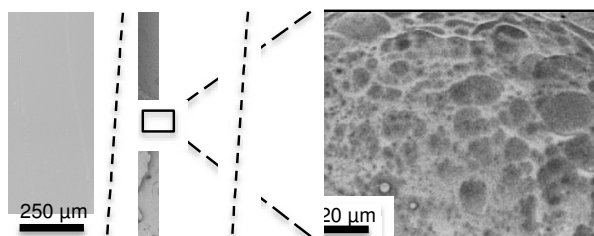
1 **Table 3. Summary of the reactions performed on the monoliths**

Step	Reagents	Conditions	Outcome
Immobilization via TE click chemistry and ASA linkage			
Photografting	200µL 2-(boc amino)ethandiol + 0.5% ^{w/v} TPO-L	UV exposure, 30 s	The monolith features t-Boc protected amino groups
Flushing	0.05% Tween 20 in DDW	5 min, 50µL/min	Removal of unreacted products
Deprotection	4 M HCl	12 h, 4µL/min	Removal of t-boc protecting group to reveal amino groups at the monolith surface
Incubation	1% ^{w/v} ASA in MeOH	30 min	Coupling of ASA to amino groups on the monoliths
Flushing	DDW	5 min, 30 µL/min	Removal of unreacted products
Incubation	Galactose Oxidase/ PNGase F	Overnight, 4°C	Coupling between immobilized ASA and the free primary amino groups of the enzymes
Flushing	DDW	5 min, 30 µL/min	Removal of unreacted groups
Immobilization via free thiols (galactose oxidase microreactor)			
Incubation	Galactose oxidase (0,14 mg/ml, 50 U/ml) in 50 mM Tris-HCl buffer, pH 8.0.	Overnight, 4°C	Reversible covalent linkage between cysteine groups on the enzyme and free thiols on the monolith
Reduction of disulfide bonds (galactose oxidase microreactor)			
Flushing	2 mM TCEP	1 h, 50µL/min	Removal of enzymes immobilized via the formation of disulfide bonds
D-Galactose Assay (galactose oxidase microreactor)			
Incubation	50 µM D-galactose, 25 µM ADHP, 0.01 U/ml HRP in tris-HCl buffer (pH 8.0)	30 min, 37°C	Oxidation of D-galactose and production of H ₂ O ₂ . Oxidation of ADHP into fluorescent resorufin
Deglycosylation of RNase B (PNGase F microreactor)			
Conditioning	50 mM ammonium bicarbonate buffer	5 min, 30 µL/min	Monolith conditioning
Deglycosylation	Ribonuclease B (1 mg/ml in 50 mM ammonium bicarbonate buffer) with 5 mM TCEP-HCl heated to 100°C for 10 min	Gentle suction applied	Collection of the deglycosylated products

2 **Results and Discussion**3 **Monolith characterization**4 **TE emulsions with water as the dispersed phase resulting in foam-like TE monoliths**

5 High internal phase TE emulsions (polyHIPEs) in which water formed 75-80% of
6 the emulsion were prepared using either Span 80 or Hypermer B246 as a
7 surfactant. As seen in Figure 3 (*Left*), the polyHIPE monoliths formed a very
8 strong bond with the channel walls and chip cover, resulting in a smooth pore-
9 free TE layer at the top of the monolith where the TE microfluidic chip cover
10 used to be. Since chips and monoliths are made out of the same material, the
11 uncured monoliths fused seamlessly with the microchannel walls, creating an
12 extremely strong anchoring upon curing. The magnified view of the monolith's
13 cross-section (Figure 3 (*Right*)) reveals that the monolith remains intact and
14 porous in its center. This type of polyHIPEs based on TE chemistry have been
15 reported previously for bulk preparations.³⁴⁻³⁸ However, the scaling down of the

1 process proved to be difficult and irreproducible for applications in microfluidic
 2 devices. PolyHIPEs form highly viscous, paste-like emulsions⁹ which are difficult
 3 to inject inside microchannels and the emulsification process can take up to
 4 60 min.³⁶ Emulsions containing various concentrations of surfactants and organic
 5 phase modifiers mixed for shorter times with an overhead mixer were unstable.
 6 Since the preparation of polyHIPEs was inconsistent with rapid, reproducible
 7 and simple monolith preparation, all subsequent experiments (characterization
 8 and enzymatic microreactors) were performed with the second type of emulsion
 9 investigated, where the TE forms the dispersed phase in methanol.

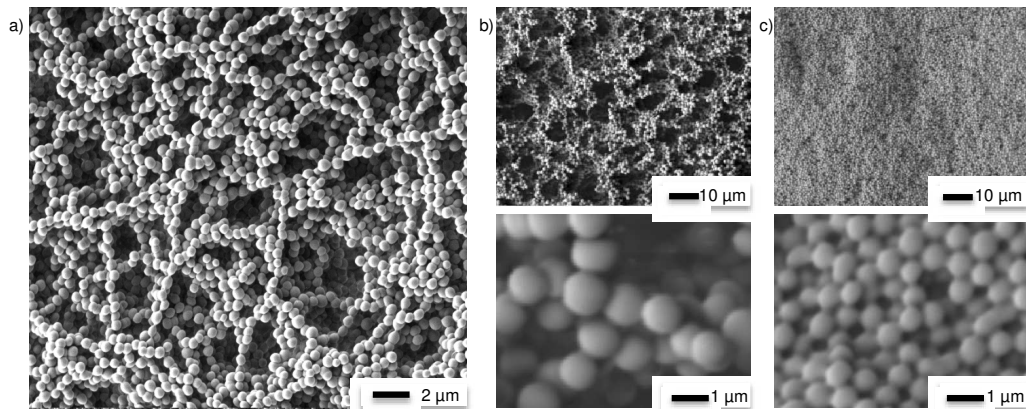


10

11 **Figure 3.** TE monolith where water forms the dispersed phase. (Left) The monolith is shown inside the
 12 channel after the top layer of the chip has been removed. Dashed lines have been added to highlight the
 13 channel walls. The upper darker half of the channel is empty. (Right) Magnified view of the monolith's cross
 14 section. The emulsion consisted of 80% water w/w while the organic phase consisted of S-TE, chloroform
 15 (50% w/w of the organic phase) Span 80 (3% w/w of organic phase) and a photoinitiator (Lucirin TPO-L, 0.2
 16 % v/v).

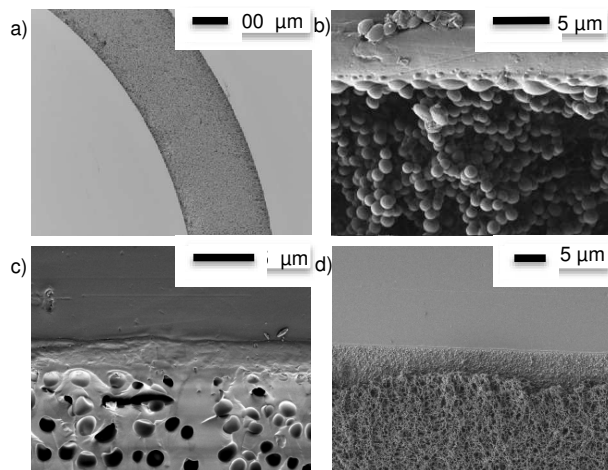
17 Emulsions with TE as the dispersed phase resulting in bead-like TE monoliths

18 The second type of emulsion proved to be more adequate for applications in
 19 microfluidic devices. This type of emulsion required less than a minute of stirring
 20 with a magnetic stir bar and resulted in a network of highly regular
 21 interconnected beads (Figure 4-a)) with interstitial macropores 0.5-5 μm in
 22 diameter depending on the preparation conditions. The emulsions were stable,
 23 showing no or little coalescence of droplets prior to curing and their low
 24 viscosity made introduction inside TE microfluidic channels possible by simple
 25 capillary action although external pressure was applied for more consistency.
 26 The size of the beads as well as the density of their packing was highly
 27 dependent upon the preparation conditions as shown in Figure 4-b) and -c),
 28 where higher stirring speeds result in smaller, more densely packed beads. No
 29 significant differences could be seen in the appearance of the monoliths based on
 30 variations in the stoichiometric composition of the TE monomers. All
 31 characterization experiments were performed on S-TE monoliths.



1
2 **Figure 4.** a) Monoliths in which TE constituted the dispersed phase in methanol (80% methanol used as a
3 porogen) formed a network of highly regular interconnected beads. b) Loosely packed larger (ca. 1 μ m)
4 beads are obtained at a lower stirring speeds (40% of maximum stirring intensity). c) Smaller (ca. 750 nm)
5 more tightly packed beads can be obtained at higher stirring speeds (60% of maximum stirring intensity).

6 As shown in Figure 5-a), the methanol/TE emulsions filled the channel
7 completely and uniformly and the TE beads fused with the microchannel
8 walls (Figure 5-b)), providing strong anchoring of the monolith. At the interface
9 between the monolith and the TE microchannel walls, a smooth TE film resulting
10 from the fusing of the beads with the wall can be observed (Figure 5-c). This
11 fusing of the monolith beads with the surrounding TE chip walls was
12 independent of the stoichiometric composition of either the TE monolith, or the
13 TE chip. Therefore, TE monoliths can be covalently anchored to TE microchannel
14 walls without any prior surface activation, independently of which stoichiometric
15 composition is used. Finally, Figure 5-d) shows that the TE monoliths did exhibit
16 shrinkage upon drying, causing cracks and detachment from the channel walls.
17 All monoliths should therefore be filled with DDW and sealed to prevent drying if
18 not used immediately.

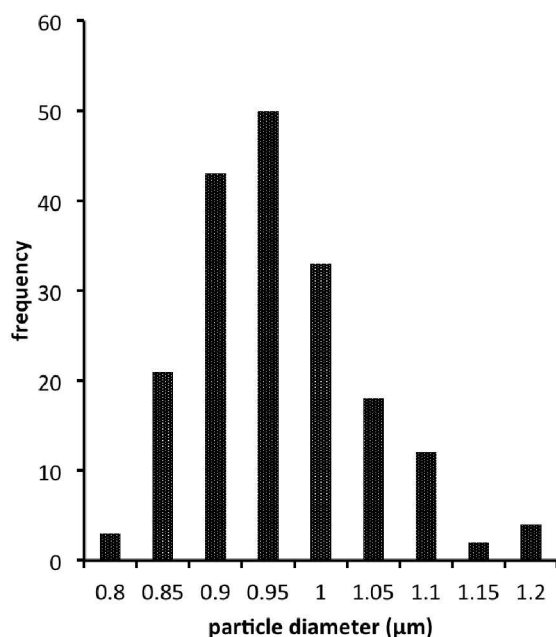


19
20 **Figure 5.** Emulsions with TE as the dispersed phase in methanol forming bead-like monoliths. The top
21 covers have been pried open and the monoliths thoroughly dried prior to imaging. All images represent a
22 top view of the channel. a) The network of beads fills up the microchannel uniformly. b) The TE beads fuse
23 seamlessly with the channel walls to provide a strong anchoring. c) Smooth TE layer observed at the
24 interface between the TE monolith and TE chip top cover. d) The monoliths exhibit slight shrinkage upon
25 drying and can break away from the chip walls.

1 **Size distribution of bead-like TE monoliths**

2 Bead uniformity and monodispersity are highly desirable for chromatographic
 3 applications. Liu *et al.* recently demonstrated that enhancing the uniform
 4 structure, rather than increasing surface area, could improve chromatographic
 5 separation for small molecules on TY globular agglomerates.⁴² Figure 6 shows a
 6 typical size distribution observed for synthesized S-TE monolith beads. The
 7 beads are highly regular with a relatively narrow particle size distribution.
 8 However, as previously shown in Figure 4, the size of the beads as well as their
 9 packing density was highly dependent on the preparation conditions. Changing
 10 the beaker shape, stir bar size or mixing speed can all have an impact on the
 11 bead size produced, with a more vigorous stirring resulting in smaller beads.
 12 Table 4 shows the average particle size measured for five different S-TE
 13 monoliths prepared under similar conditions. Although the distributions are
 14 narrow, the means of the 5 populations are statistically different, highlighting the
 15 sensitivity of the process.

16



17

18 **Figure 6.** Typical bead size distribution for a bead-like S-TE monolith prepared using 80% w/w methanol as
 19 the porogen

20 **Table 4.** Population distribution for five bead-like S-TE monoliths prepared using 80% w/w methanol as the
 21 porogen

	Average size* (µm)
Sample 1	1,4 ± 0,2
Sample 2	0,98 ± 0,08
Sample 3	1,2 ± 0,2
Sample 4	1,05 ± 0,07
Sample 5	1,2 ± 0,1

22 * Standard deviations are reported for N=119-241

1 **Specific surface area of bead-like TE monoliths**

2 The specific surface area of the monoliths prepared with 80% and 60% methanol
3 were $2.1 \pm 0.6 \text{ m}^2 \cdot \text{g}^{-1}$ and $1.8 \pm 0.6 \text{ m}^2 \cdot \text{g}^{-1}$, respectively. The small surface area
4 indicates that the material was macroporous, with no or little micro- or
5 mesopores.⁴¹ However, since the monoliths were cured in bulk rather than
6 inside a TE microchannel and that they exhibit considerable shrinkage upon
7 drying, the results obtained by Kr BET analysis are not an exact representation of
8 the surface area of the monoliths prepared in much smaller quantities inside TE
9 microfluidic channels. Still, the results are consistent with those obtained by *Liu*
10 *et al.*⁴¹ for similar organic-inorganic hybrid TE monoliths used successfully in
11 capillary based liquid chromatography.

12 **Galactose assay using the galactose oxidase enzymatic microreactor**

13 Galactose oxidase was immobilized on OSTE-allyl monoliths (40% excess ene)
14 via TE click chemistry and ASA linkage. Additionally, the enzyme was incubated
15 on unmodified OSTE-thiol, OSTE-allyl and S-TE monoliths to promote
16 immobilization via disulfide bridges and to measure the magnitude of adsorption
17 and non-specific interactions between the enzyme and the various TE monoliths.
18 The term “unmodified” is used to describe monoliths without any prior surface
19 treatment or modification, where a simple incubation was used to immobilize
20 the enzyme of interest. As shown in Figure S 1, the microreactors featuring
21 enzymes immobilized via click chemistry and ASA linkage were significantly
22 more efficient at converting the non-fluorescent ADHP into the fluorescent
23 resorufin product than the unmodified TE microreactors. However, more in-
24 depth investigations are necessary to determine whether the higher efficiency is
25 due to a higher activity or a higher immobilization density of the ASA-
26 immobilized enzyme on the monolith.

27 The presence of immobilized galactose oxidase on the unmodified TE
28 monoliths is likely due to the formation of disulfide bonds between the free thiol
29 groups present on the galactose oxidase cysteine side-chain and the thiol groups
30 present at the surface of the TE monolith. Similarly, the irreversible adsorption
31 of proteins (trypsin, cytochrome c, lysozyme, myoglobin and β -lactoglobulin) on
32 thiol-functionalized SBA-15 molecular sieves has been reported previously by Yu
33 *et al.*^{49,50} The assay results reported in Figure S 1 indicate that a significant
34 amount of enzyme was immobilized at the surface of OSTE-thiol and S-TE
35 monoliths, but also to a smaller extent at the surface of OSTE-allyl monoliths.
36 These results indicate the likely presence of free unconverted thiol groups on S-
37 TE and OSTE-allyl monoliths. Ellman’s reagent (DTNB) was used to evaluate the
38 thiol group density at the surface of TE substrates with various stoichiometric
39 compositions. As seen in Figure S 2, a significant number of free thiol groups are
40 indeed present at the surface of S-TE polymers and even on OSTE-allyl polymers.
41 Typically, in stoichiometric formulations it is expected that the thiol and ene
42 components of the mixture will be consumed at identical rates. However, it is
43 unlikely that monomer conversion is 100%, so some leftover functional groups
44 are expected at the surface of the monoliths. Additionally, homopolymerization
45 of the ene monomers can alter the polymerization stoichiometry, leading to a
46 higher conversion of the ene functional groups compared to the thiol functional
47 groups.⁵¹ Cramer *et al.*⁵¹ have demonstrated that the conversion of the ene

1 functional groups can be as much as 15% greater than that of the thiol functional
2 group for the triallyl and tetrathiol monomers used here. These conversion
3 results are consistent with the assay results reported in Figure S 1.

4 ***Reduction of disulfide bonds for enzyme removal TE monoliths***

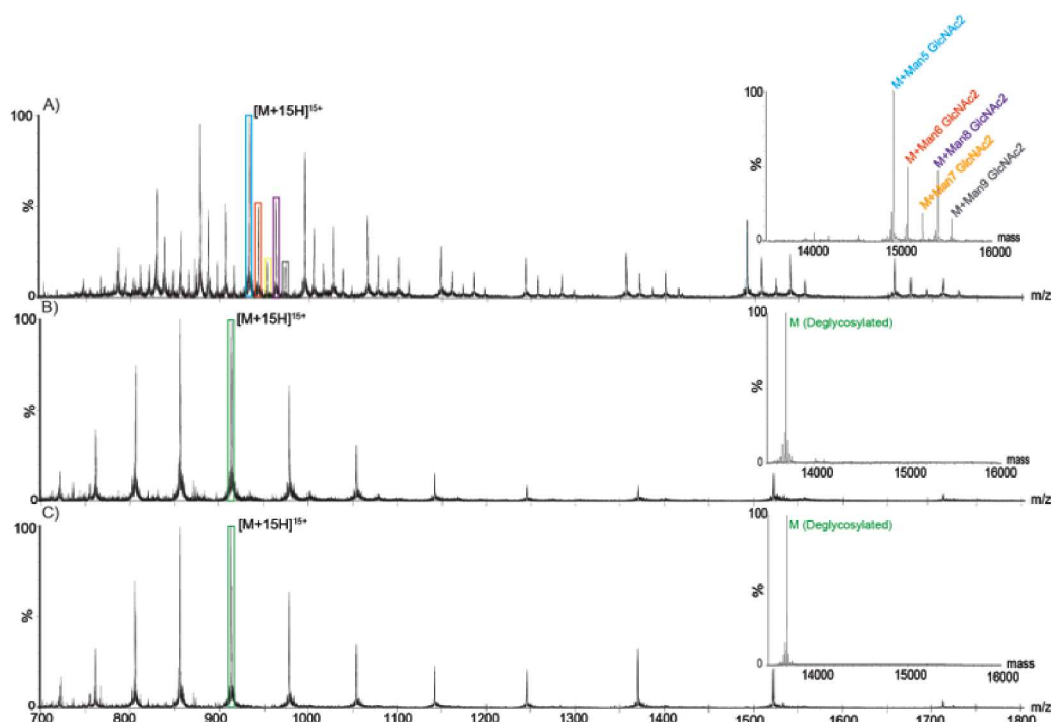
5 Enzymes that were immobilized on the support only via a disulfide bond can
6 be eluted from the by incubation with TCEP, a reducing agent typically used to
7 break disulfide bonds. After thorough flushing of the reactors with TCEP, most
8 enzymes had been removed from the unmodified TE monoliths, with a
9 conversion of ADHP into the fluorescent resorufin product down by 75-81%. In
10 contrast, the OSTE-allyl monoliths in which the enzymes had been immobilized
11 via click chemistry and ASA linkage could not be regenerated via reduction with
12 TCEP. A fluorescence intensity of 81% of the original value could still be obtained
13 for the conversion of ADHP into the fluorescent resorufin after thorough flushing
14 with TCEP. Therefore, the ASA linkage provides a strong, irreversible covalent
15 immobilization of the enzyme while immobilization via disulfide bonds on
16 unmodified TE monoliths featuring free thiol groups allows for easy
17 regeneration of the monoliths.

18 ***Storage stability of the galactose-oxidase enzymatic microreactor***

19 Although enzymatic reactors featuring galactose oxidase immobilized via click
20 chemistry and ASA linkage could be re-used immediately with minimal decrease
21 in activity, even after thorough flushing with TCEP, enzyme activity decreased
22 significantly during storage as shown in **Error! Reference source not found..**
23 Similar trends were observed both for never-used and re-used enzymatic
24 microreactors after up to 13 days of storage in DDW at 4°C. Results indicate that
25 optimally, the microreactors should be used within 4 days of their preparation.
26 However, optimization of the storage conditions could improve the microreactor
27 stability over time.

28 ***Deglycosylation of RNase B using the PNGase F enzymatic microreactor***

29 PNGase F is a deglycosylation enzyme, which cleaves N-linked carbohydrates.
30 The activity of immobilized PNGase F was assessed using RNase B as a substrate.
31 RNase B contains a single N-linked glycan at residue 60 and MS analysis of a
32 reference sample of native glycosylated RNase B showed the presence of five
33 high-mannose RNase B glycoforms (with a structure of two N-
34 acetylglucosamines- and five to nine mannose monosaccharides). MS analysis of
35 a reference sample of RNase B deglycosylated off-chip showed a single mass at
36 13692 Da, corresponding to the fully deglycosylated form of the protein. As
37 shown in Figure 7, RNase B samples processed with PNGase F both on- and off-
38 chip yielded similar spectra, corresponding to the fully deglycosylated protein
39 and the absence of any of the native glycoforms. Furthermore, similar on-chip
40 deglycosylation was observed for chips employing either strategy for PNGase F
41 immobilization.



1
2 **Figure 7.** On-chip deglycosylation of RNase B measured by LC-MS. A) Mass spectrum of glycosylated RNase
3 B. $[M+15H]^{15+}$ is colored to indicate the five charge state distributions corresponding to the native
4 glycoforms of RNase B. The corresponding deconvoluted spectrum is shown in the insert using the same
5 coloring scheme. B) Mass spectrum of RNase B deglycosylated off-chip by PNGase F. $[M+15H]^{15+}$ is colored to
6 indicate the charge state distribution of the deglycosylated form of RNase B. The corresponding
7 deconvoluted spectrum is shown in the insert using the same coloring scheme. C) Mass spectrum of RNase B
8 deglycosylated online by PNGase F immobilized on a microfluidic chip via TE click chemistry and ASA
9 linkage. $[M+15H]^{15+}$ is colored to indicate the charge state distribution of the deglycosylated form of RNase
10 B. The corresponding deconvoluted spectrum is shown in the insert using the same coloring scheme.

11 Conclusions

12 Thiol-ene microfluidic platforms featuring emulsion-templated porous
13 monoliths show promise for applications such as enzyme microreactors, where a
14 large surface area is necessary and it is paramount that the enzyme is strongly
15 bound to the solid support. Highly uniform and monodisperse bead-like thiol-
16 ene monoliths were prepared inside microfluidic channels. Curing and
17 anchoring inside the microchannel was achieved in a single, rapid photoinitiated
18 step without any prior surface modification. We have shown that immobilization
19 of enzymes on the prepared monoliths via the formation of disulfides is
20 straightforward and reversible. Alternatively, enzymes can be covalently and
21 irreversibly immobilized via the free amino groups in their primary structure by
22 means of ASA linkage. The prepared galactose oxidase and PNGase F
23 microreactors demonstrated good enzymatic activity in a galactose assay and the
24 deglycosilation of RNase B, respectively. The prepared monoliths also offer
25 promise as stationary phases for on-chip separations thanks to their narrow size
26 distribution and the possibility to easily modify their surfaces with chemical
27 groups for various retention modes.

1 Acknowledgments

2 Funding for this project was provided by the Danish Council for Independent
3 Research – Technology and Production (Grant No DFF- 4005-00341). Author S.S.
4 acknowledges funding from Denmark's Advanced Technology Foundation (Grant
5 No 144-2013-6). Authors J.N. and G.N. gratefully acknowledge funding by the
6 Erasmus program. Author J.N. acknowledges funding by the Grant Office project
7 (GROFF, CZ.1.07/2.4.00/17.0106) and the Grant Agency of the Czech Republic
8 (project P20612G014). Author K.D.R. acknowledge funding from the Marie Curie
9 Actions Programme of the EU (Grant No. PCIG09-GA-2011-294214) and the
10 Danish Council for Independent Research – Natural Sciences (Steno Fellowship
11 No. 11-104058). We acknowledge the Core Facility for Integrated Microscopy,
12 Faculty of Health and Medical Sciences, University of Copenhagen as well as
13 Dorthe Orbæk from the Department of Pharmacy (University of Copenhagen) for
14 her help with SEM imaging. Finally we would like to thank Denis Okhrimenko
15 from the NanoGeoscience Center (University of Copenhagen) for performing the
16 surface area analyses.

17 References

- 18 1 J. Krenkova and F. Foret, *ELECTROPHORESIS*, 2004, **25**, 3550–3563.
19 2 F. Svec, *ELECTROPHORESIS*, 2006, **27**, 947–961.
20 3 J. Krenkova and F. Svec, *J. Sep. Sci.*, 2009, NA–NA.
21 4 F. Svec and A. A. Kurganov, *J. Chromatogr. A*, 2008, **1184**, 281–295.
22 5 J. Krenkova, F. Foret and F. Svec, *J. Sep. Sci.*, 2012, **35**, 1266–1283.
23 6 F. Svec, *J. Chromatogr. B*, 2006, **841**, 52–64.
24 7 S. Xie, R. W. Allington, J. M. J. Fréchet and F. Svec, *Adv. Biochem. Eng.*
25 *Biotechnol.*, 2002, **76**, 87–125.
26 8 H. Zhang and A. I. Cooper, *Soft Matter*, 2005, **1**, 107.
27 9 M. S. Silverstein, *Polymer*, 2014, **55**, 304–320.
28 10 C. Harrison, J. T. Cabral, C. M. Stafford, A. Karim and E. J. Amis, *J.*
29 *Micromechanics Microengineering*, 2004, **14**, 153–158.
30 11 P. Wägli, A. Homsy and N. F. de Rooij, *Sens. Actuators B Chem.*, 2011, **156**,
31 994–1001.
32 12 L.-H. Hung, R. Lin and A. P. Lee, *Lab. Chip*, 2008, **8**, 983.
33 13 B. Levaché, A. Azioune, M. Bourrel, V. Studer and D. Bartolo, *Lab. Chip*, 2012,
34 **12**, 3028–3031.
35 14 S. H. Kim, Y. Yang, M. Kim, S. -w Nam, K. -m Lee, N. Y. Lee, Y. S. Kim and S.
36 Park, *Adv. Funct. Mater.*, 2007, **17**, 3493–3498.
37 15 E. P. Dupont, R. Luisier and M. A. M. Gijs, *Microelectron. Eng.*, 2010, **87**, 1253–
38 1255.

- 1 16 S. Silvestrini, D. Ferraro, T. Tóth, M. Pierno, T. Carofiglio, G. Mistura and M.
2 Maggini, *Lab. Chip*, 2012, 4041–4043.
- 3 17 B. T. Good, S. Reddy, R. H. Davis and C. N. Bowman, *Sens. Actuators B Chem.*,
4 2007, **120**, 473–480.
- 5 18 V. S. Khire, Y. Yi, N. A. Clark and C. N. Bowman, *Adv. Mater.*, 2008, **20**, 3308–
6 3313.
- 7 19 C. F. Carlborg, T. Haraldsson, K. Öberg, M. Malkoch and W. van der Wijngaart,
8 *Lab Chip*, 2011, **11**, 3136–3147.
- 9 20 J. P. Lafleur, R. Kwapiszewski, T. G. Jensen and J. P. Kutter, *The Analyst*, 2013,
10 **138**, 845–849.
- 11 21 N. A. Feidenhans'l, J. P. Lafleur, T. G. Jensen and J. P. Kutter,
12 *ELECTROPHORESIS*, 2014, **35**, 282–288.
- 13 22 F. Saharil, C. F. Carlborg, T. Haraldsson and W. van der Wijngaart, *Lab. Chip*,
14 2012, **12**, 3032.
- 15 23 T. M. Sikanen, J. P. Lafleur, M.-E. Moilanen, G. Zhuang, T. G. Jensen and J. P.
16 Kutter, *J. Micromechanics Microengineering*, 2013, **23**, 037002.
- 17 24 C. E. Hoyle and C. N. Bowman, *Angew. Chem. Int. Ed.*, 2010, **49**, 1540–1573.
- 18 25 A. B. Lowe, *Polym. Chem.*, 2010, **1**, 17.
- 19 26 A. B. Lowe, C. E. Hoyle and C. N. Bowman, *J Mater Chem*, 2010, **20**, 4745–
20 4750.
- 21 27 P. Thirumurugan, D. Matosiuk and K. Jozwiak, *Chem. Rev.*, 2013.
- 22 28 Y.-X. Chen, G. Triola and H. Waldmann, *Acc Chem Res*, 2011, **44**, 762–773.
- 23 29 P. Jonkheijm, D. Weinrich, M. Köhn, H. Engelkamp, P. C. M. Christianen, J.
24 Kuhlmann, J. C. Maan, D. Nüsse, H. Schroeder, R. Wacker, R. Breinbauer, C. M.
25 Niemeyer and H. Waldmann, *Angew. Chem. Int. Ed.*, 2008, **120**, 4421–4424.
- 26 30 V. Grazú, O. Abian, C. Mateo, F. Batista-Viera, R. Fernández-Lafuente and J. M.
27 Guisán, *Biotechnol. Bioeng.*, 2005, **90**, 597–605.
- 28 31 Y.-H. Rogers, P. Jiang-Baucom, Z.-J. Huang, V. Bogdanov, S. Anderson and M. T.
29 Boyce-Jacino, *Anal. Biochem.*, 1999, **266**, 23–30.
- 30 32 M. T. Neves-Petersen, T. Snabe, S. Klitgaard, M. Duroux and S. B. Petersen,
31 *Protein Sci. Publ. Protein Soc.*, 2006, **15**, 343–351.
- 32 33 W. W. Cleland, *Biochemistry (Mosc.)*, 1964, **3**, 480–482.
- 33 34 E. Lovelady, S. D. Kimmins, J. Wu and N. R. Cameron, *Polym. Chem.*, 2011, **2**,
34 559–562.
- 35 35 S. Caldwell, D. W. Johnson, M. P. Didsbury, B. A. Murray, J. J. Wu, S. A.
36 Przyborski and N. R. Cameron, *Soft Matter*, 2012, **8**, 10344.
- 37 36 B. Sergent, M. Birot and H. Deleuze, *React. Funct. Polym.*, 2012, **72**, 962–966.
- 38 37 L. Kircher, P. Theato and N. R. Cameron, *Polymer*, 2013, **54**, 1755–1761.
- 39 38 C. R. Langford, D. W. Johnson and N. R. Cameron, *Polym Chem*, 2014, **5**, 6200–
40 6206.

- 1 39 X. Gong, W. Wen and P. Sheng, *Langmuir*, 2009, **25**, 7072–7077.
- 2 40 R. A. Prasath, M. T. Gokmen, P. Espeel and F. E. D. Prez, *Polym. Chem.*, 2010, **1**,
3 685–692.
- 4 41 Z. Liu, J. Ou, H. Lin, Z. Liu, H. Wang, J. Dong and H. Zou, *Chem. Commun.*, 2014,
5 **50**, 9288–9290.
- 6 42 Z. Liu, J. Ou, H. Lin, H. Wang, Z. Liu, J. Dong and H. Zou, *Anal. Chem.*, 2014, **86**,
7 12334–12340.
- 8 43 S. Brunauer, P. H. Emmett and E. Teller, *J. Am. Chem. Soc.*, 1938, **60**, 309–319.
- 9 44 G. L. Ellman, *Arch. Biochem. Biophys.*, 1959, **82**, 70–77.
- 10 45 P. W. Riddles, R. L. Blakeley and B. Zerner, in *Enzyme Structure Part I*,
11 Academic Press, 1983, vol. Volume 91, pp. 49–60.
- 12 46 A. J. D. Magenau, J. W. Chan, C. E. Hoyle and R. F. Storey, *Polym. Chem.*, 2010, **1**,
13 831.
- 14 47 A. Patton and P. Chism, *Anal. Chem.*, 1951, **23**, 1683–1685.
- 15 48 T. J, B. P and K. D, 1999.
- 16 49 H. H. P. Yiu, C. H. Botting, N. P. Botting and P. A. Wright, *Phys. Chem. Chem.*
17 *Phys.*, 2001, **3**, 2983–2985.
- 18 50 H. H. P. Yiu, P. A. Wright and N. P. Botting, *J. Mol. Catal. B Enzym.*, 2001, **15**,
19 81–92.
- 20 51 N. B. Cramer and C. N. Bowman, *J. Polym. Sci. Part Polym. Chem.*, 2001, **39**,
21 3311–3319.
- 22
- 23